Supporting Information

Unveiling Ultrafast Dynamics in Bridged Bimetallic Complexes Using Optical and X-ray Transient Absorption Spectroscopies

Michael W. Mara,[1,2] Brian T. Phelan,[1] Zhu-Lin Xie,[1] Tae Wu Kim,[1] Darren J. Hsu,[1,2] Xiaolin Liu,[3] Andrew J. S. Valentine,[3] Pyosang Kim,[1,2] Xiaosong Li,[3] Shin-ichi Adachi,[4,5] Tetsuo Katayama,[6,7] Karen L. Mulfort,[1] Lin X. Chen[1,2]

[1]Chemical Sciences and Engineering Division, Argonne National Laboratory, Lemont, Illinois 60437 USA

[2]Department of Chemistry, Northwestern University, Evanston, Illinois 60208, USA

[3]Department of Chemistry, University of Washington, Seattle, Washington 98195, USA

[4]Institute of Materials Structure Science, High Energy Accelerator Research Organization (KEK), 1-1 Oho, Tsukuba, Ibaraki 305-0801, Japan.

[5]Department of Materials Structure Science, School of High Energy Accelerator Science, The Graduate University for Advanced Studies, 1-1 Oho, Tsukuba, Ibaraki 305-0801, Japan

[6]Japan Synchrotron Radiation Research Institute, Kouto 1-1-1, Sayo, Hyogo 679-5198, Japan.

[7]RIKEN SPring-8 Center, 1-1-1 Kouto, Sayo, Hyogo 679-5148, Japan.

CuOs XTA – Long-Time Kinetic Traces

In order to determine the Cu and Os excited-state lifetimes in **CuOs**, kinetics traces were collected with 3 ps step size out to 150 ps time delay. Kinetics are shown in Figure S14. The Cu K-edge kinetics were fit with an exponential convoluted with a Gaussian, along with an additional Gaussian function (to model the sub-ps kinetics) and a shelf. A 49 ps lifetime is obtained for the excited-state decay, with a long-lived shelf. For Os, a bi-exponential convoluted Gaussian function is used; the first time constant models the <2 ps components shown in Figure 5a, while the second has a lifetime >>150 ps time range used in the measurement. This is consistent with the OTA measurements that expected a ~400 ps excited-state decay for **CuOs** at both 500 nm and 625 nm excitation.

CuOs XTA – 500 nm vs. 625 nm Excitation

XTA spectra of **CuOs** were measured with two excitation wavelengths: 500 nm, where a mixture of Cu and Os MLCT are excited, and 625 nm, where predominantly Os MLCT is excited. The XTA spectra at the Cu K- and Os L_{III}-edges are shown in Figure S13. The same general difference signal observed with 500 nm excitation is observed here. Although absorption at 625 nm mostly originates from Os MLCT absorption, a small tail from the Cu MLCT band allows direct excitation of the Cu MLCT state. Kinetics traces were measured following 625 nm excitation, using the same incident energies used in Figure 5a. The kinetics at the two excitation wavelengths are plotted together in Figure S18. The Os kinetics at 625 nm overlays quite well with the 500 nm kinetics trace, showing that the MLCT dynamics are consistent between the two pump wavelengths. It is more difficult to judge the Cu MLCT kinetics because those obtained with the 625 nm excitation because the difference signal is much weaker, but the rise and decay of the kinetics appears consistent with the 500 nm excitation.

XTA Experimental Time Resolution

The time resolution of the XTA measurement, similar to optical measurements, is dependent on both temporal width of both the X-ray and optical laser pulses. However, due to the non-stochastic nature of the generation of the X-ray pulses, a timing tool is used to correct the arrival time for the X-rays, and the bin size chosen will further impact the time resolution. Additionally, the group velocity dispersion mismatch of optical and X-ray pulses through liquid media will introduce further temporal broadening. Assuming ~50 fs FWHM optical and X-ray pulses, 50 fs timing tool bin size, and 100 µm liquid jet, our predicted experimental time resolution is

$$IRF = \sqrt{(50^2) + (50^2) + (50^2) + (100^2)} = 132 \text{ fs} \quad [1]$$

To gain an experimental estimate of the instrument response, the derivative of the kinetics traces at the Cu K- and Os L_{III}-edges was fit to a Gaussian response, shown in Figure S2. The fits yielded an IRF of ~120 fs at the Cu K-edge and ~140 fs at the Os L_{III}-edge, showing that our effective time resolution is consistent with our predicted value. This is consistent with the method used by Katayama et al.[1]

Cu K-edge XTA Residual Fitting

As discussed in the main text, oscillations are observed in the XTA residuals, assigned as coherent vibrational wavepackets. These are modelled using a sum of damped sine waves:

$$\sum A_i * \ sin(\pi * \frac{(t - t_{c,i})}{w_i}) * exp^{(}\frac{(t - t_{c,i})}{\tau_i}) \quad [1]$$

where damped sine waves with dephasing time τ_i and period w_i are centered in time at $t_{c,I}$ with amplitude A_i. Data in the main text are fit to a single component, with the total fitting results shown in Table S3. The weak amplitude of the oscillations makes it difficult to reliably extract a dephasing time; however, the 40 cm^{-1} frequency is consistent both with the ISRS measurements, and the rise time in the XTA (half the period of the 40 cm^{-1} mode.)

CuOs Computational Results – Molecular Orbitals and Vibrational Modes

DFT calculations were used to generate molecular orbitals (Mos) for **CuOs**, as well as determine the nature of the low frequency vibrational modes that appear in the ISRS/XTA. Computational details are shown in Experimental. MOs for the HOMO, LUMO, and LUMO + 1 are shown in Figure S16. The HOMO is largely localized on the Os center and the surrounding ligands, while the LUMO and LUMO + 1 are largely delocalized across the tpphz bridging ligand. This demonstrates that upon photoexcitation, electron density will ultimately be distributed across the bridging ligand in close proximity to both the Cu and Os centers.

ISRS measurements of **CuOs** revealed vibrational modes of ~50, 240 and 430 cm^{-1}. To assign these vibrations, ground-state Raman modes were calculated for **CuOs**, with representative modes shown in Figure S17 - Figure S19. The 430 cm^{-1} vibrational mode likely corresponds to breathing modes on the tpphz ligand at the Cu and Os centers, as shown in the 431 and 443 cm^{-1} modes, respectively. There are two calculated modes that could likely represent the experimental 240 cm^{-1} mode. At 232 cm^{-1}, distortions are seen in the rotation of the Cu HETPHEN center which involves modulating π-stacking interactions between the tpphz ligand and the mesityl group at the phenanthroline 2,9 positions. At 238 cm^{-1}, a large breathing mode in the tpphz ligand is observed, causing expansion of the tpphz ligands while altering the Os-N and Cu-N bond distances. Finally, the 60 cm^{-1} vibrational mode detected by ISRS likely corresponds to an additional tpphz breathing mode (calculated at 58 cm^{-1}), similar to that at 238 cm^{-1}. Importantly, both the experimental 50 and 240 cm^{-1} modes can be ascribed to breathing modes in the tpphz ligands, which serve to cause alterations in the metal-ligand bonding distance, which should cause the vibrational modes to manifest in the XTA kinetics. The 240 cm^{-1} is difficult to observe via XTA, however, as the period of this vibrational mode is approaching the time-resolution of that measurement, and the 50 fs step size used would cause such an oscillatory feature to be under-sampled.

Cyclic Voltammetry

Cyclic voltammetry was used to determine the redox potentials for the Cu and Os centers in **CuOs** and **OsOs**, with the results plotted in Figure S15. **CuOs** and **OsOs** have nearly identical potentials for the Os^{+2}/Os^{+3} couple around 900 mV. **CuOs** exhibits a Cu^{+1}/Cu^{+2} couple around 540 mV. Therefore, **CuOs** should have ~360 mV driving force for hole transfer from the Os to the Cu. This is similar to the driving force for hole transfer observed in the previously published **CuH_2-$CuMe_2$**,[2] which is also a tpphz-bridged complex. Relevant redox potentials for **CuOs**, **OsOs**, and related complexes are shown in Table S2.

XTA – Laser Power Titration

Laser power scans were performed to determine the linear/non-linear optical absorption regimes, shown in Figure S1. Difference signal is linear in pulse energy until ~15 μJ; 14.37 μJ pulse energy used in experiments, giving fluence of ~80 mJ/cm^2.

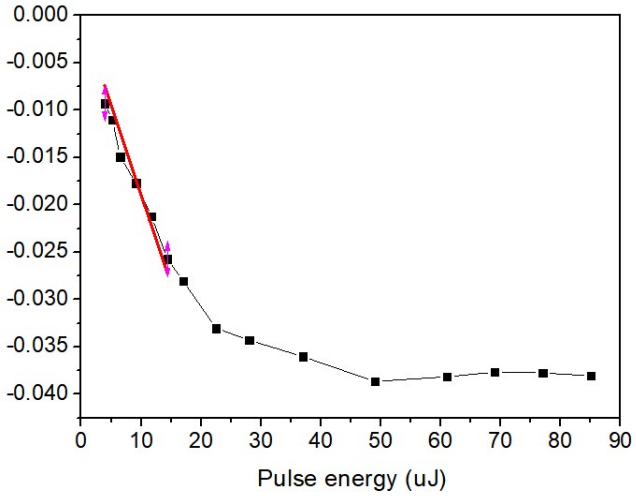

Figure S1: Power titration curve measured at the Cu K-edge with 500 nm excitation. X-ray energy is 8.986 keV

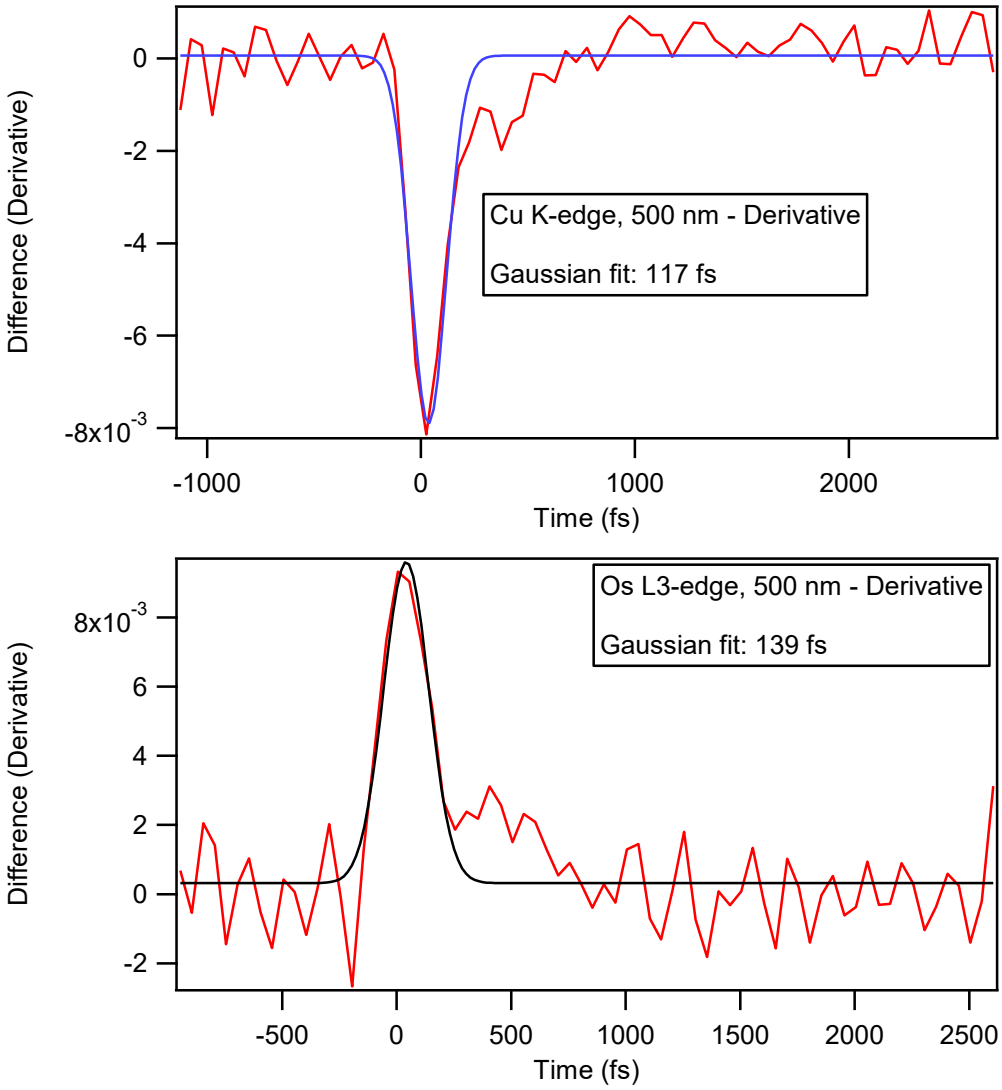

Figure S2: Derivative of Cu K-edge (top) and Os L_{III}-edge (bottom) kinetics traces. Derivative was fit to Gaussian to estimate experimental time resolution.

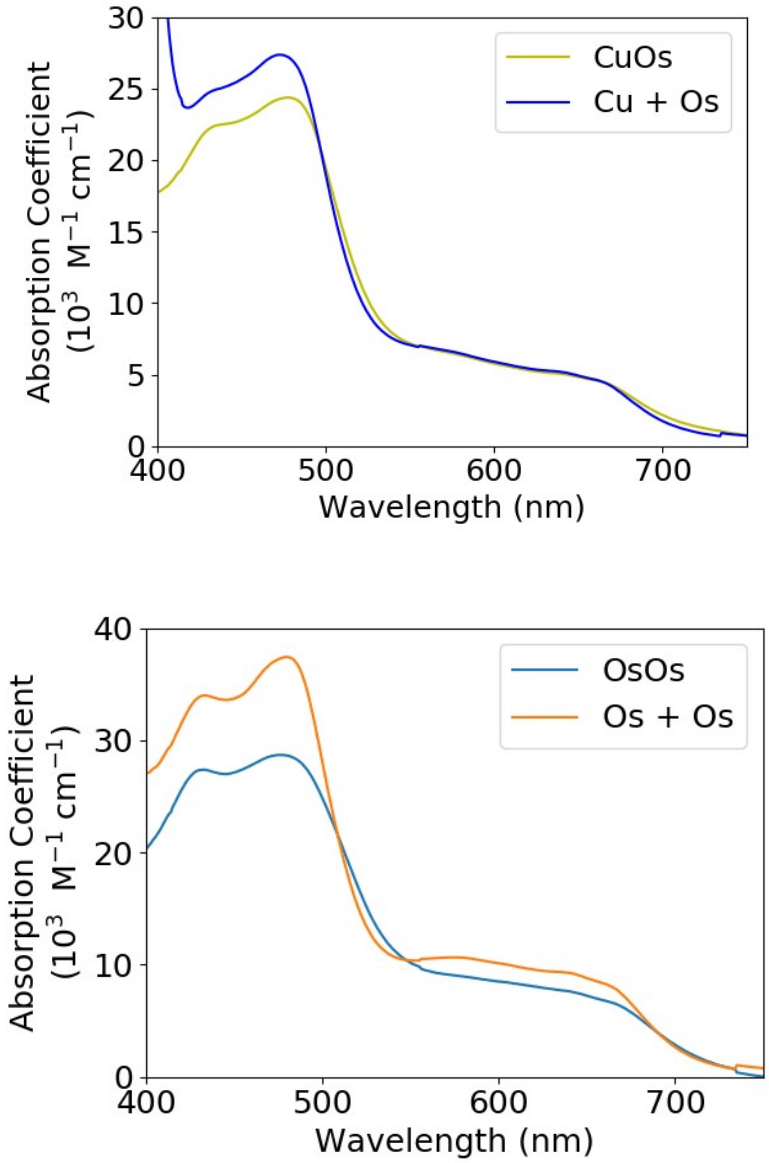

Figure S3: Top: UV-Vis of **CuOs** compared with the sum of **Cu** and **Os** spectra. Bottom: UV-Vis of **OsOs** compared with the sum of two **Os** spectra.

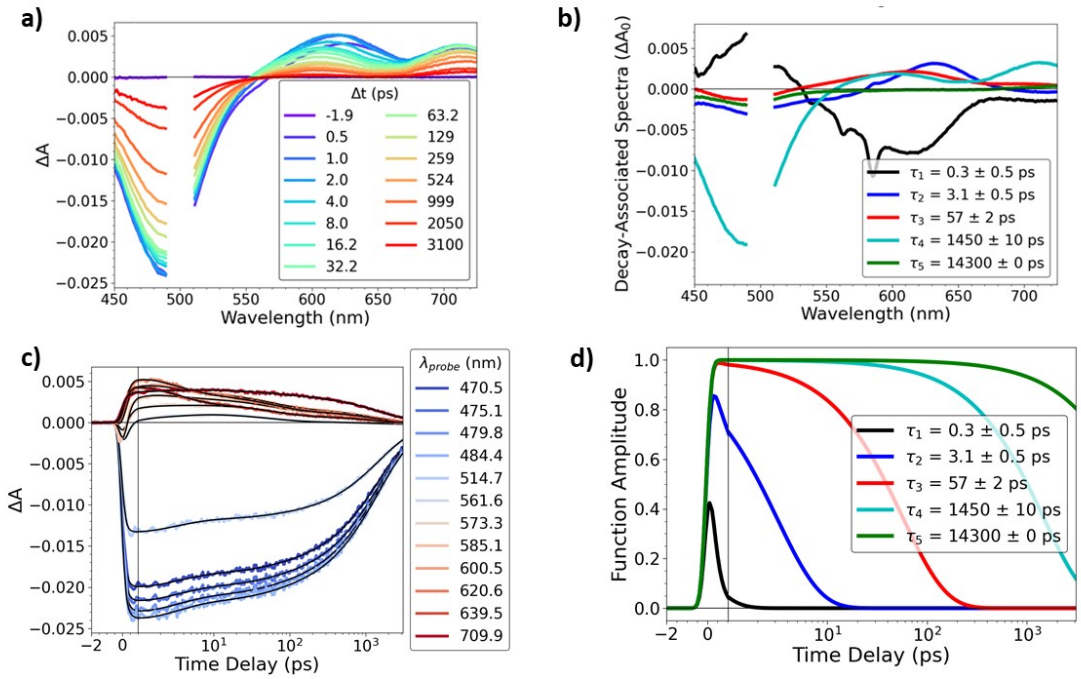

Figure S4: OTA spectra of **CuOs** following 500 nm excitation. a) Individual spectra; b) decay-associated spectra; c) individual kinetics traces; d) amplitude decay curves. These are consistent with the data in Figure 2A, but include the additional fit impurity component (as τ_5)

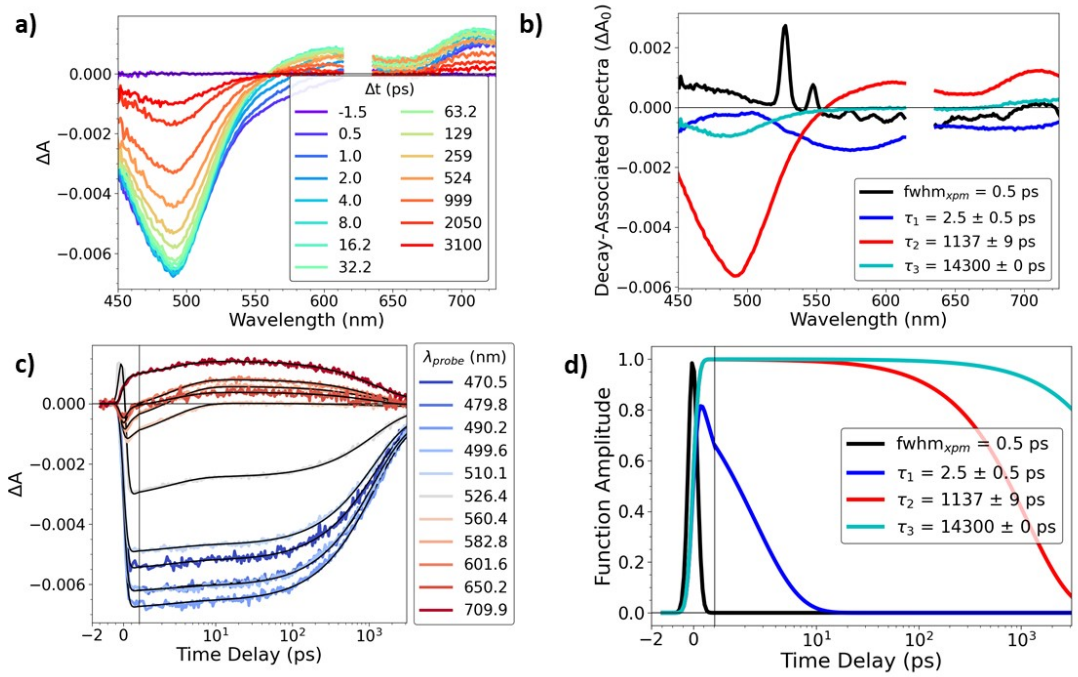

Figure S5: OTA spectra of **CuOs** following 625 nm excitation. a) Individual spectra; b) decay-associated spectra; c) individual kinetics traces; d) amplitude decay curves

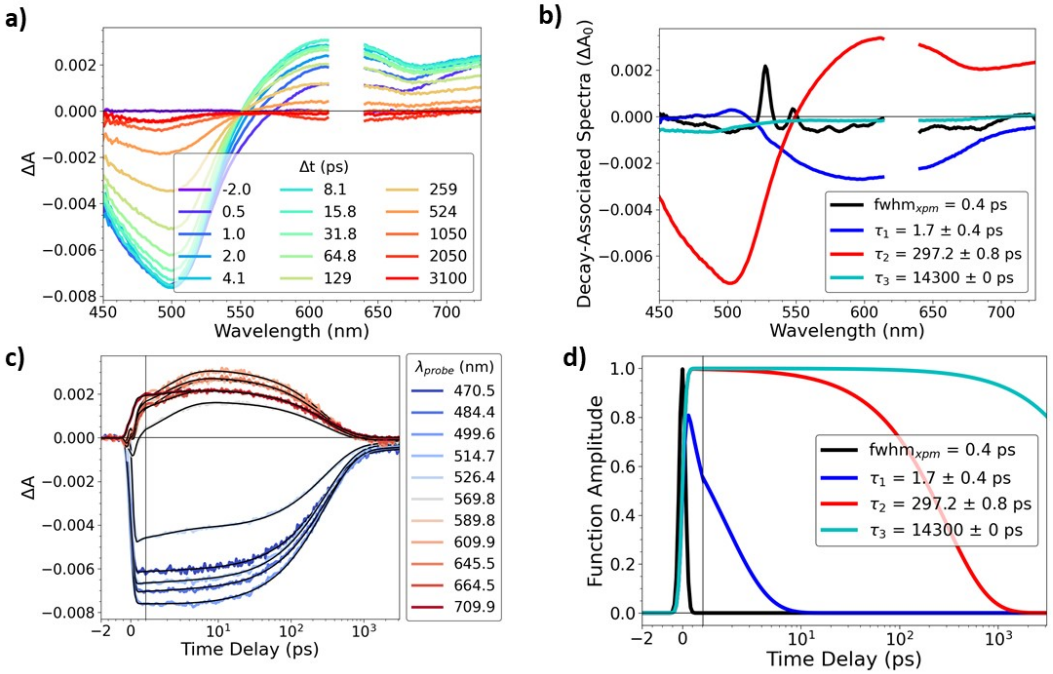

Figure S6: OTA spectra of **OsOs** following 625 nm excitation. a) Individual spectra; b) decay-associated spectra; c) individual kinetics traces; d) amplitude decay curves

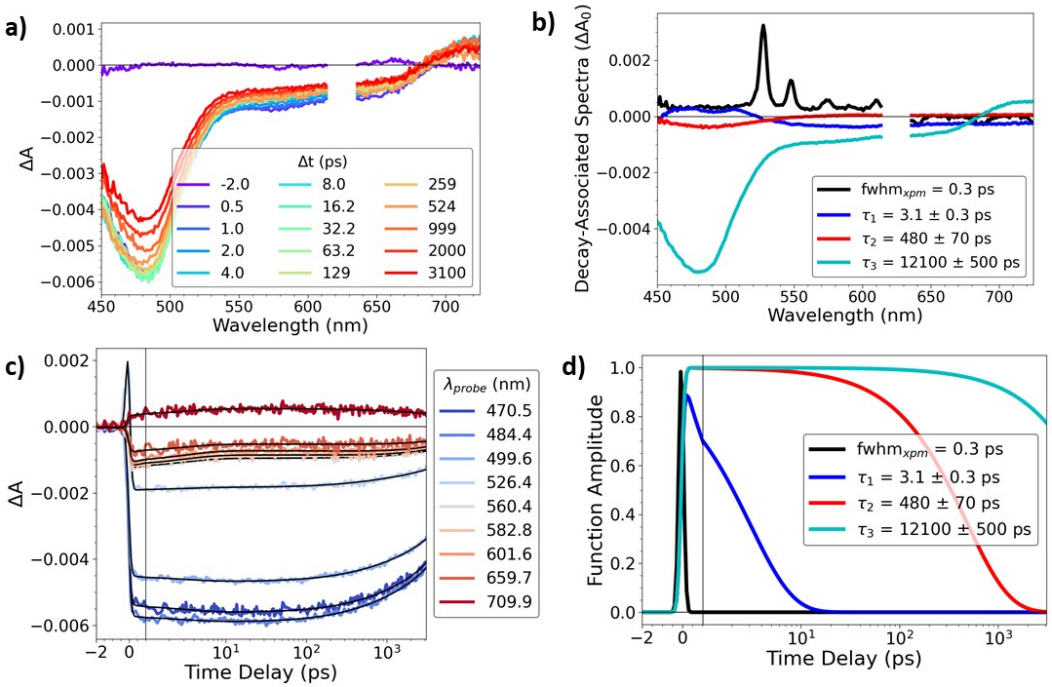

Figure S7: OTA spectra of **Os** following 625 nm excitation. a) Individual spectra; b) decay-associated spectra; c) individual kinetics traces; d) amplitude decay curves

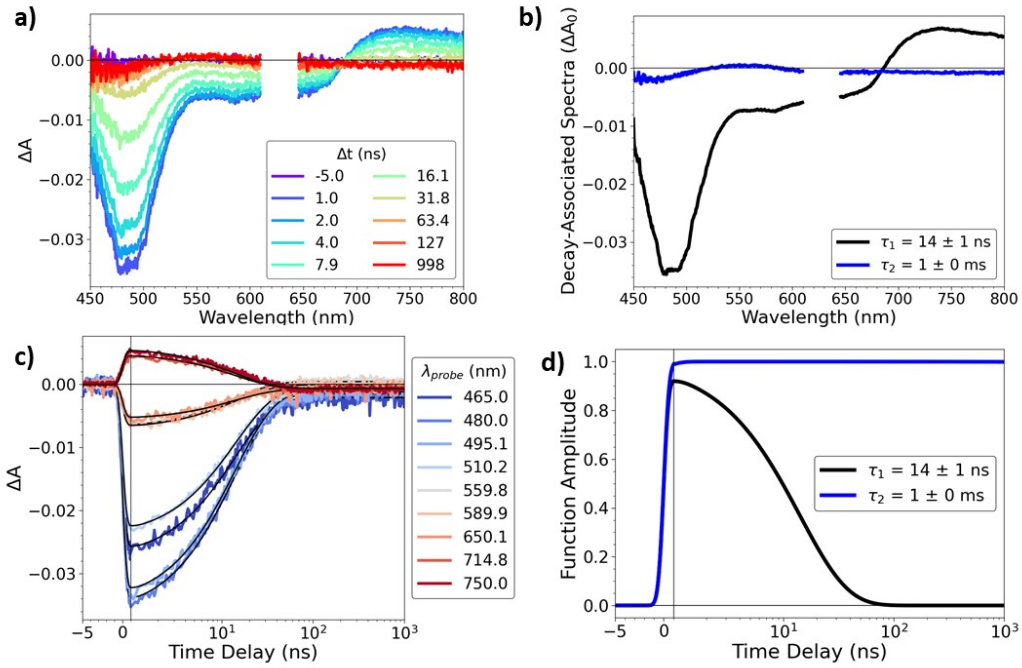

Figure S8: nsOTA spectra of **Os** following 625 nm excitation. a) Individual spectra; b) decay-associated spectra; c) individual kinetics traces; d) amplitude decay curves

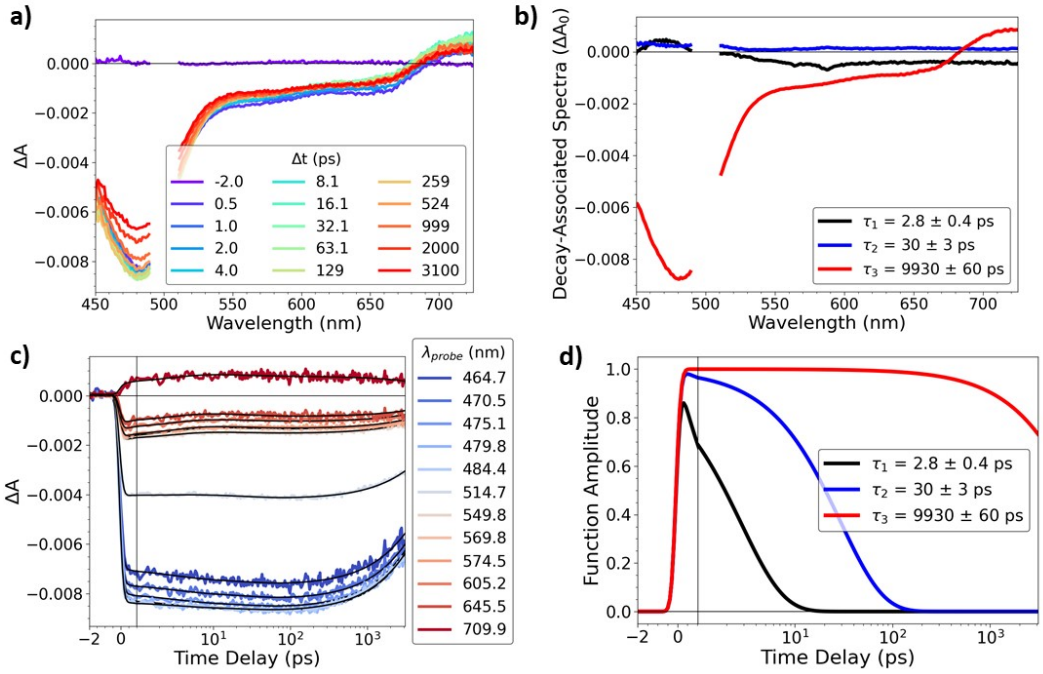

Figure S9: OTA spectra of **Os** following 500 nm excitation. a) Individual spectra; b) decay-associated spectra; c) individual kinetics traces; d) amplitude decay curves

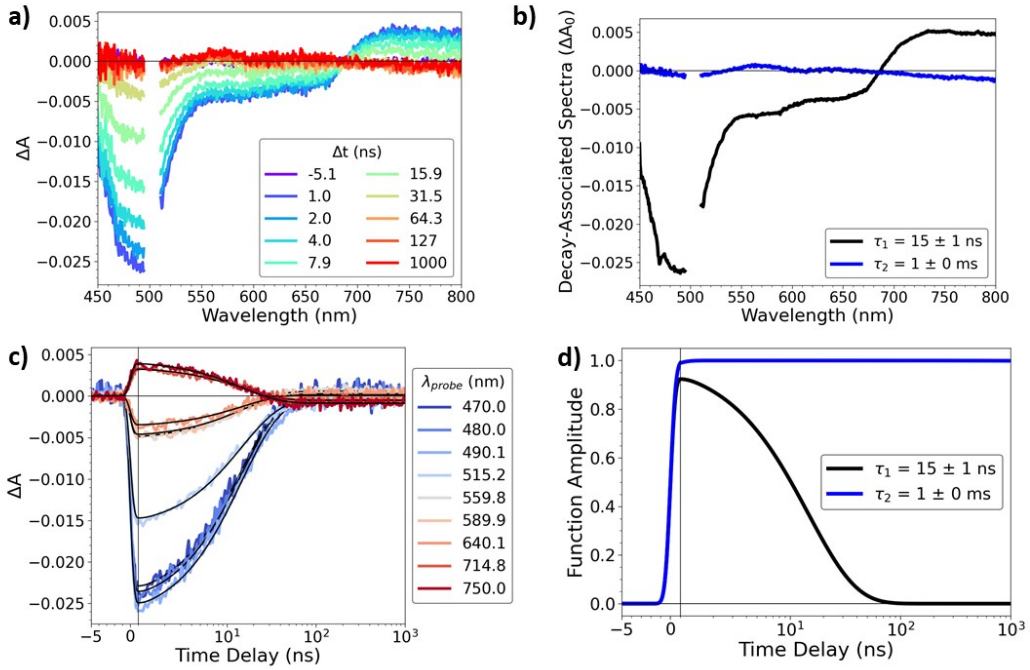

Figure S10: nsOTA spectra of **Os** following 500 nm excitation. a) Individual spectra; b) decay-associated spectra; c) individual kinetics traces; d) amplitude decay curves

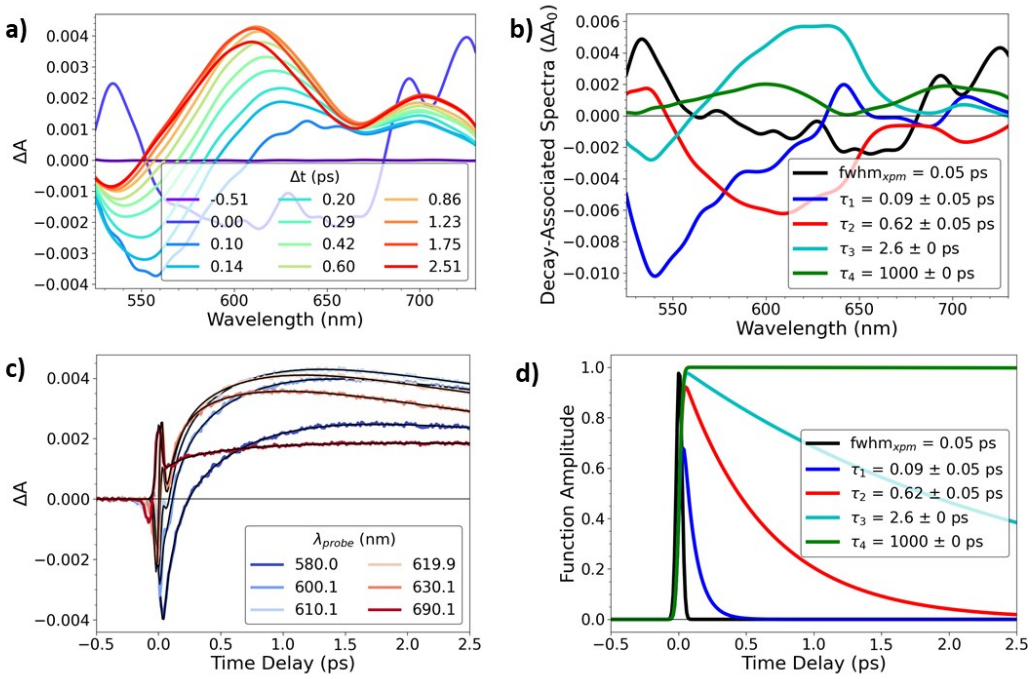

Figure S11: ISRS spectra for **CuOs** following 540 nm excitation. a) Individual spectra; b) decay-associated spectra; c) individual kinetics traces; d) amplitude decay curves

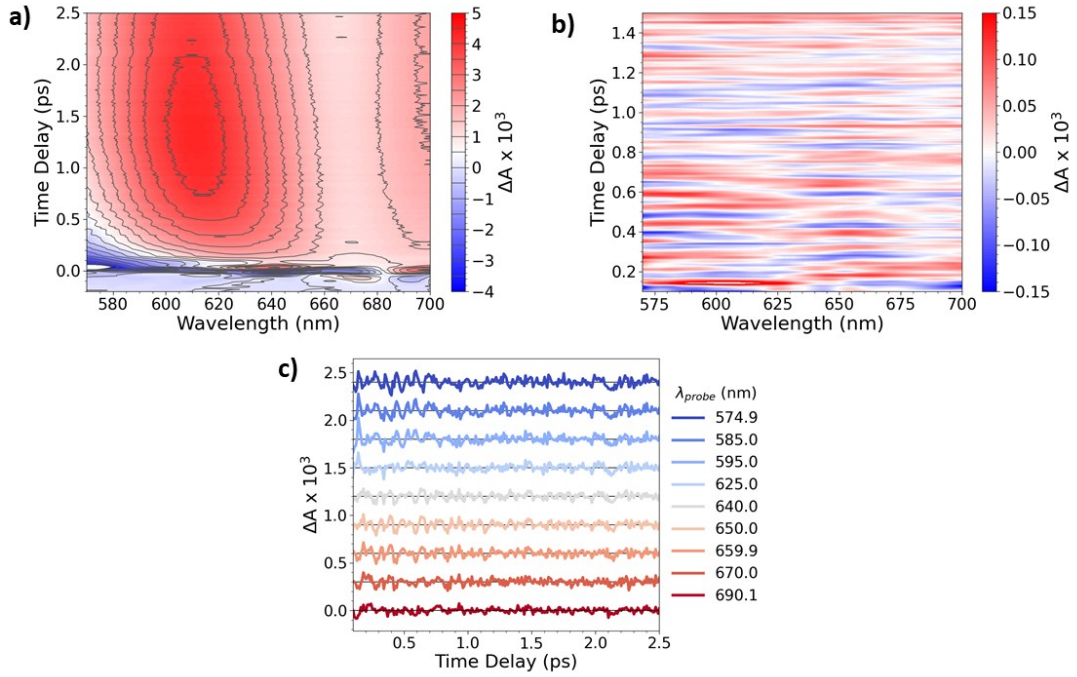

Figure S12: a) ISRS data before subtraction of multiexponential fit (described in Figure S11.) Residuals are shown as 2D plot (b) and in individual wavelength cuts (c)

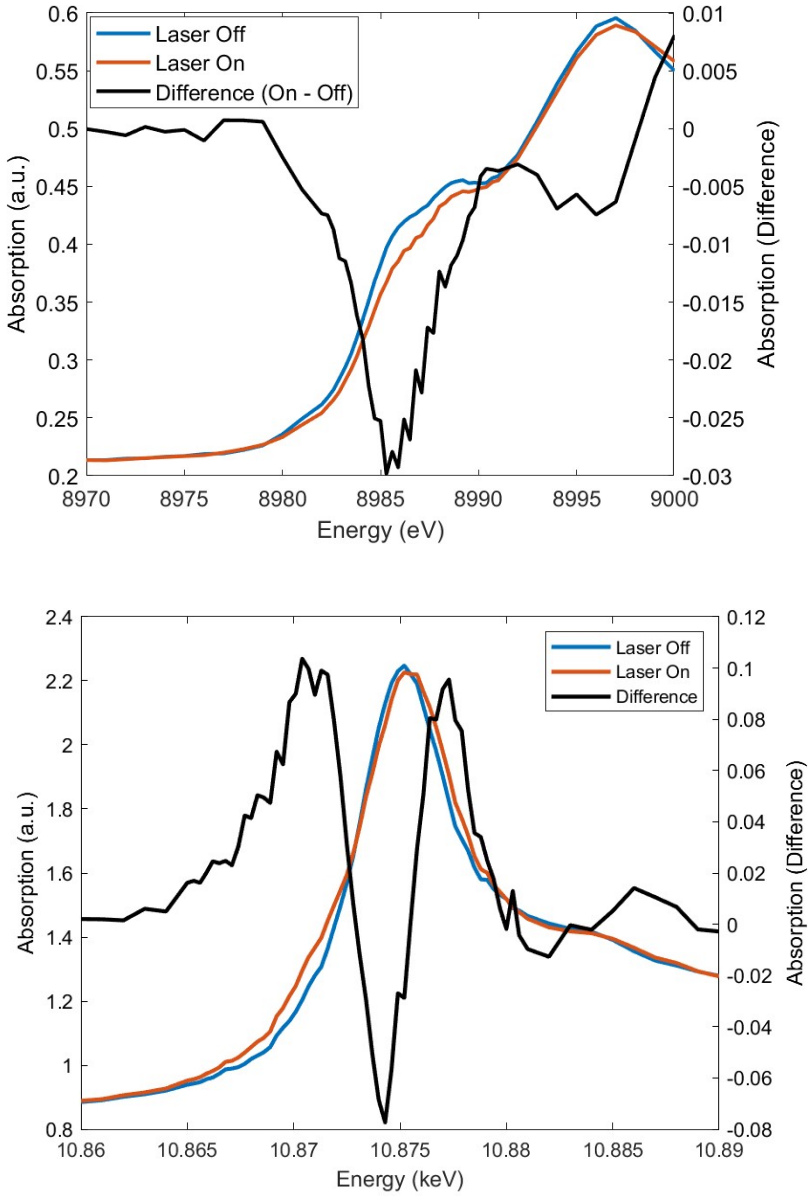

Figure S13: Cu K-edge (top) and Os L_{III}-edge (bottom) XTA spectra following 625 nm excitation. Spectra collected at 13 ps and 5 ps time delays, respectively.

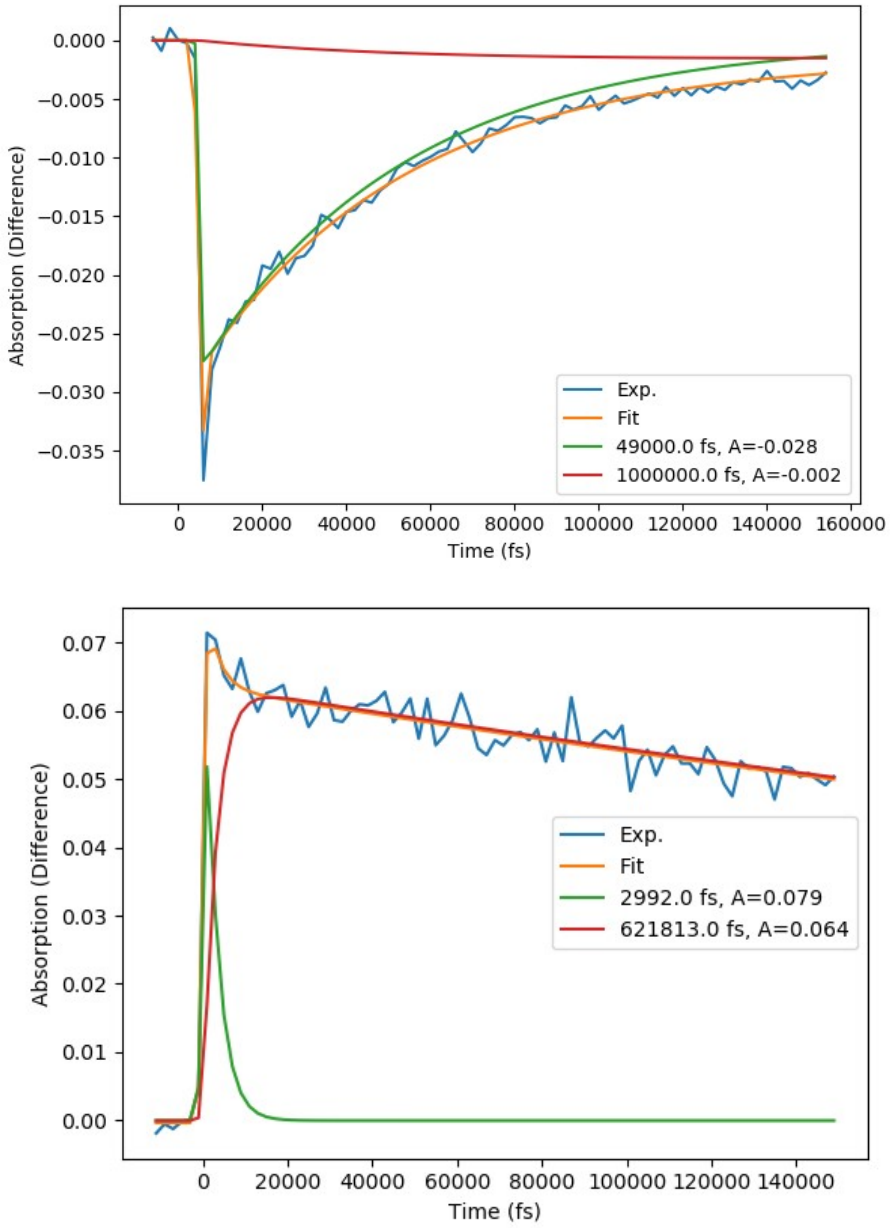

Figure S14: XTA kinetics traces at the Cu K (top) and Os L_{III} (bottom) edges, following the excited-state decay at each metal center. Cu exhibits an excited-state decay time of ~49 ps (with a small, long-lived component), while the Os exhibits a >>150 ps excited-state decay, consistent with the **CuOs** OTA measurements.

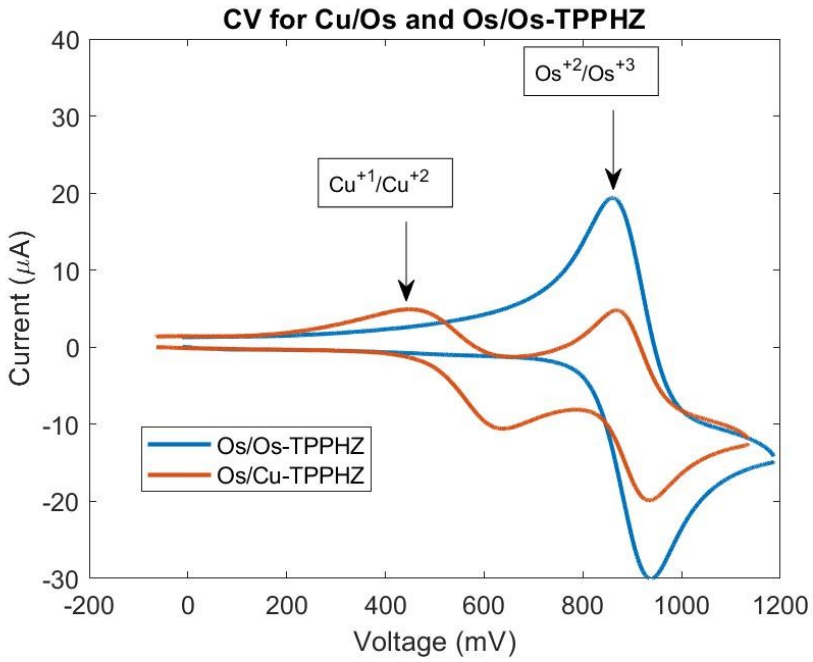

Figure S15: Cyclic voltammogram for **CuOs** in acetonitrile

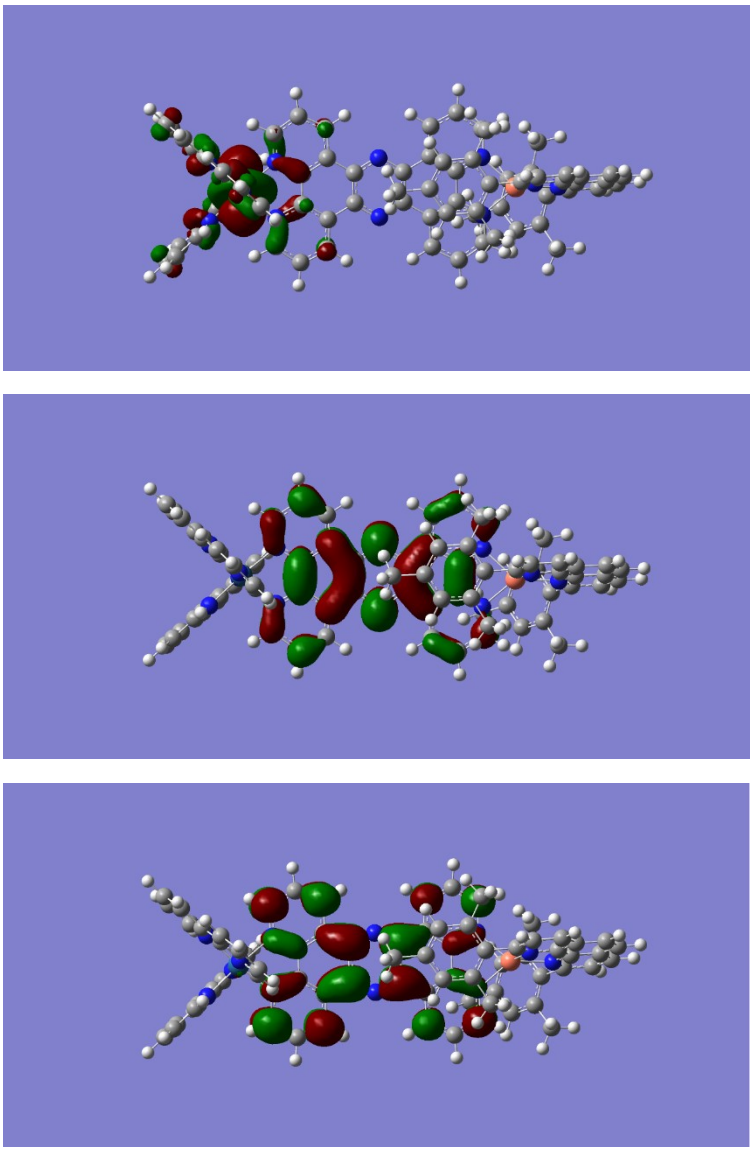

Figure S16: Orbital Diagrams of the HOMO, LUMO, and LUMO + 1 for CuOs

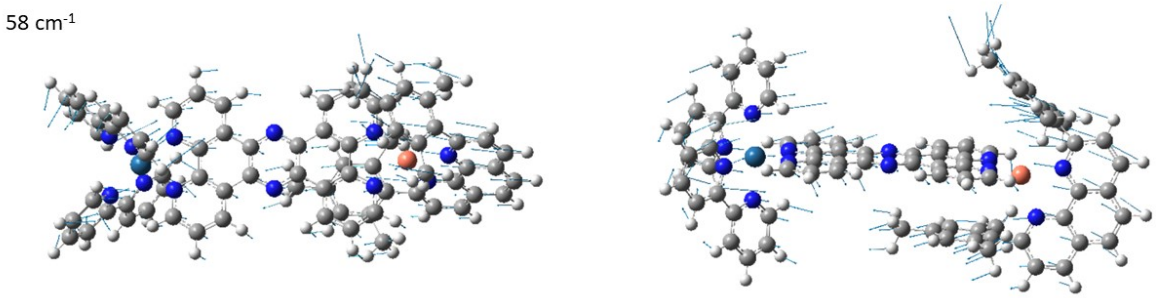

Figure S17: Calculated 58 cm-1 vibrational mode

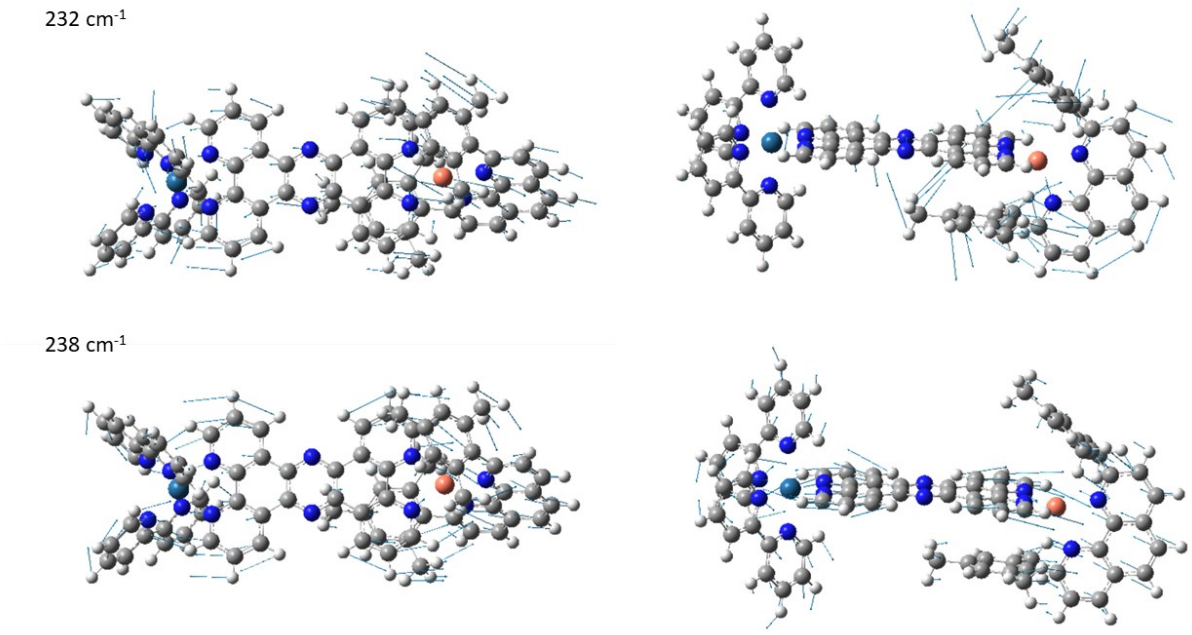

Figure S18: Calculated vibrational modes at 232 cm^{-1} and 238 cm^{-1}

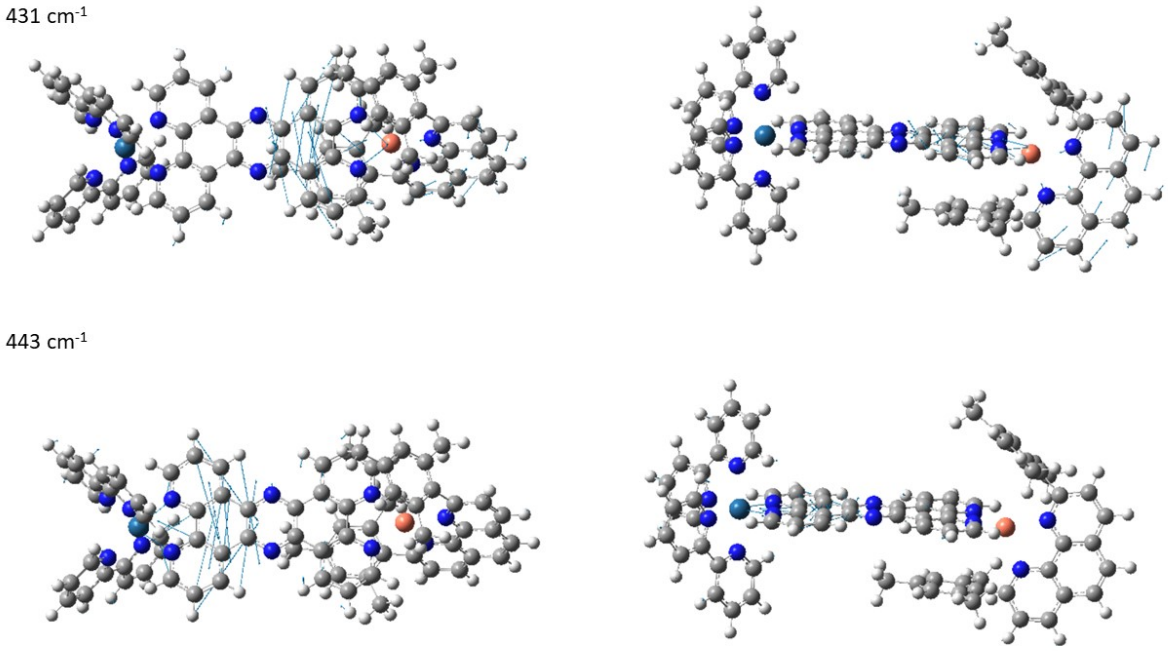

Figure S19: Calculated 431 cm^{-1} and 443 cm^{-1} vibrational modes

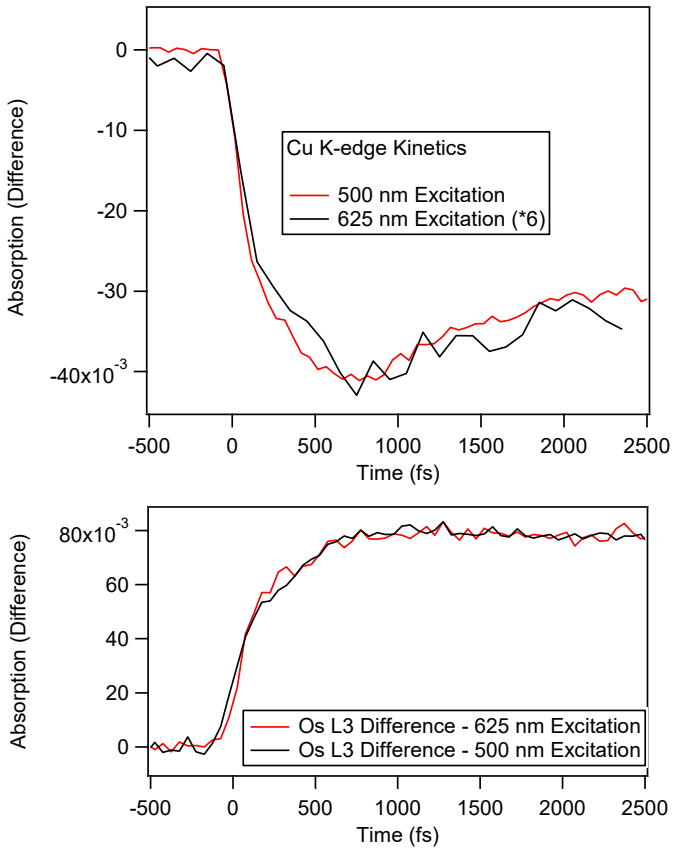

Figure S20: Kinetics at Cu K-edge (top) and Os L_{III}-edge (bottom) at 500 nm excitation (black) and 625 nm excitation (red)

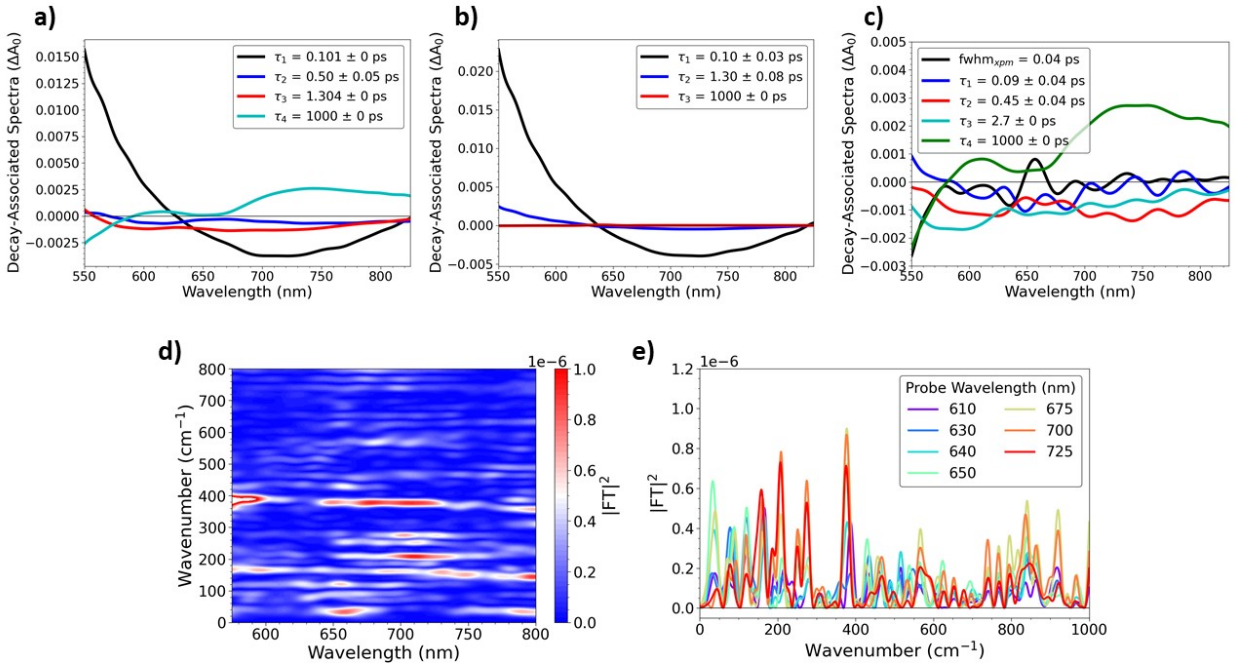

Figure S21: ISRS for **CuOs** (a) following 640 nm excitation. Solvent response (b) is subtracted from a) to generate c); data were scaled based on intensity of DAS1 in a) and b), and fit with same model used for 540 nm ISRS. d) ISRS spectrum. e) FT Raman spectra at selected wavelength from d)

Table S1: Fitting Parameters for ISRS measurements of **CuOs**		
	540 nm excitation	640 nm excitation
τ_1 (ps)	0.088	0.09
τ_2 (ps)	0.625	0.45
τ_3 (ps)[a]	2.6	2.7
τ_4 (ps)[a]	1000	1000

[a]fixed time constants

Table S2: Fitting parameters for Cu K-edge residuals	
A_1	-0.0014
τ_1 (fs)	1268
w_1 (fs)	429
$t_{c,1}$ (fs)	-290

Table S3: Cyclic Voltammagram Potentials For M_1M_2-tpphz Complexes (vs. SCE)		
Sample	Cu^{+1}/Cu^{+2} (mV)	M^{n+}/M^{n+1} (mV)
CuOs	540	900
OsOs	-	899
CuH_2-$CuMe_2$[2]	570	880
$CuMe_2$-Ru[2]	890	1340

Table 4: CuOs DFT Coordinates (in Angstroms)			
Atom	X	Y	Z
C	-4.78446	-1.09383	2.43088
H	-5.77156	-1.3432	2.80062
C	-3.63776	-1.40113	3.16166
H	-3.73858	-1.90518	4.11503
C	-2.39523	-1.05758	2.66249
H	-1.4842	-1.28012	3.20564
C	-2.32419	-0.40612	1.42565
C	-3.51504	-0.13689	0.74987
C	-3.51342	0.53273	-0.52993
C	-4.77642	1.35644	-2.28464
H	-5.76065	1.50042	-2.7134
C	-3.62855	1.79505	-2.94294
H	-3.72657	2.29345	-3.89956
C	-2.38809	1.5847	-2.37027
H	-1.47562	1.90771	-2.85765
C	-2.32092	0.9375	-1.13104
C	-1.06403	0.66147	-0.44221
C	-1.06551	0.00229	0.80984
C	1.21196	0.09794	0.86428
N	0.07549	1.03288	-1.02069
C	1.21365	0.75805	-0.3897
C	2.47493	1.11446	-1.0278
C	2.52855	1.7679	-2.26652
H	1.60608	2.04733	-2.76284
C	3.76034	2.03831	-2.82813
H	3.84573	2.54647	-3.78111
C	4.91223	1.62852	-2.15166
H	5.89662	1.80409	-2.57185
N	4.87562	0.99982	-0.9814
C	3.67964	0.76178	-0.4106
C	3.67785	0.09775	0.89401
C	4.90536	-0.80192	2.61955
H	5.8898	-1.01808	3.02202
C	3.75044	-1.16214	3.3196
H	3.83312	-1.66382	4.27631
C	2.52045	-0.8698	2.76621
H	1.5962	-1.13429	3.26726
C	2.47115	-0.22038	1.52543
C	10.6628	-0.35938	0.16035
C	9.26833	-0.47665	0.0454
C	8.67422	-1.75502	-0.27057
C	7.48267	-4.13084	-0.87488
H	6.96669	-5.05339	-1.11688
C	8.85455	-4.09457	-0.7601

H	9.44544	-4.99319	-0.91047
C	9.49829	-2.87804	-0.44817
C	10.92279	-2.73289	-0.31199
H	11.54768	-3.60987	-0.44986
C	11.48011	-1.52863	-0.02274
H	12.55683	-1.42829	0.07314
N	8.43323	0.57227	0.2043
C	8.92451	1.78102	0.45229
C	10.31037	1.99066	0.58649
H	10.68099	2.98802	0.79464
C	11.17311	0.92461	0.44802
H	12.24481	1.06586	0.55056
C	7.89575	2.85825	0.5321
C	7.16516	3.03671	1.71456
C	6.0933	3.93073	1.70934
H	5.51966	4.07085	2.62307
C	5.73198	4.63368	0.56067
C	6.48802	4.44799	-0.59842
H	6.21909	4.99115	-1.50205
C	7.5664	3.56664	-0.63423
C	7.50359	2.24989	2.95666
H	6.89564	2.57469	3.80512
H	8.55901	2.36099	3.22902
H	7.32113	1.18028	2.79984
C	8.33653	3.34754	-1.91379
H	8.32779	2.29045	-2.20619
H	9.38735	3.63923	-1.80618
H	7.90726	3.93005	-2.73344
C	4.53407	5.54974	0.55151
H	3.69686	5.08304	0.01858
H	4.75807	6.49294	0.04267
H	4.19731	5.77881	1.56667
C	-8.58024	-0.22882	2.07505
H	-8.36948	0.82468	2.20983
C	-9.56862	-0.86628	2.80503
H	-10.1486	-0.30208	3.52514
C	-9.79122	-2.2223	2.59257
H	-10.5572	-2.75319	3.1462
C	-9.01639	-2.89127	1.65567
H	-9.1779	-3.94631	1.47554
C	-8.03781	-2.19562	0.95254
C	-7.16015	-2.80703	-0.06204
C	-7.19389	-4.15381	-0.41016
H	-7.88909	-4.8293	0.07157
C	-6.32592	-4.63109	-1.382
H	-6.34227	-5.67837	-1.66124

C	-5.44056	-3.74583	-1.98702
H	-4.74507	-4.07192	-2.75074
C	-5.45481	-2.41729	-1.59881
H	-4.78747	-1.69172	-2.04678
C	-8.43403	-0.02714	-2.20902
H	-8.06873	-1.03998	-2.32274
C	-9.44647	0.46931	-3.01174
H	-9.88806	-0.16696	-3.76904
C	-9.87214	1.77942	-2.82194
H	-10.6634	2.2004	-3.43159
C	-9.26802	2.54547	-1.83508
H	-9.58971	3.56594	-1.67151
C	-8.25419	1.99051	-1.06024
C	-7.54569	2.71306	0.01183
C	-7.78797	4.04168	0.34685
H	-8.52822	4.61883	-0.19219
C	-7.06977	4.62888	1.37878
H	-7.24906	5.6634	1.64843
C	-6.12153	3.8696	2.05565
H	-5.53759	4.28404	2.86839
C	-5.92425	2.55341	1.67528
H	-5.19971	1.92406	2.17664
N	-4.73417	-0.47205	1.24732
N	-4.72959	0.73138	-1.10249
N	0.07233	-0.26454	1.44596
N	4.87379	-0.19055	1.44067
N	7.32987	-1.80121	-0.38861
N	-7.82415	-0.87224	1.16761
N	-6.29389	-1.94828	-0.6579
N	-7.84317	0.71088	-1.25227
N	-6.61706	1.97847	0.67588
Cu	6.43692	0.10357	0.05722
C	6.7349	-2.95042	-0.68004
C	5.24551	-2.91866	-0.78067
C	4.63612	-2.32217	-1.89621
C	3.24372	-2.25081	-1.94071
H	2.76798	-1.78334	-2.80041
C	2.44904	-2.75812	-0.91228
C	3.08113	-3.33786	0.18776
H	2.47766	-3.72046	1.0081
C	4.47037	-3.43004	0.2715
C	5.11682	-4.05926	1.48166
H	4.38875	-4.19059	2.28666
H	5.93827	-3.44472	1.86497
H	5.53546	-5.04406	1.24332
C	5.46207	-1.77718	-3.03582

H	6.15414	-1.00202	-2.6912
H	4.82152	-1.34142	-3.80731
H	6.06608	-2.5662	-3.49905
C	0.94381	-2.71322	-1.00273
H	0.60141	-1.84114	-1.56975
H	0.48462	-2.68414	-0.00971
H	0.56061	-3.60375	-1.515
Os	-6.34331	0.02317	0.01349

References

1. Katayama, T., et al., Tracking multiple components of a nuclear wavepacket in photoexcited Cu(I)-phenanthroline complex using ultrafast X-ray spectroscopy. *Nature Communications* **2019,** *10* (1), 3606.
2. Hayes, D.; Kohler, L.; Hadt, R. G.; Zhang, X.; Liu, C.; Mulfort, Karen L.; Chen, L. X., Excited state electron and energy relays in supramolecular dinuclear complexes revealed by ultrafast optical and X-ray transient absorption spectroscopy. *Chemical Science* **2018,** *9* (4), 860-875.